

# Wet-Chemical Processing of Transparent and Antiglare Conducting ITO Coating on Plastic Substrates

M.A. AEGERTER\* AND N. AL-DAHOUDI

*Institut für Neue Materialien gGmbH, Im Stadtwald, Geb. 43, D-66123 Saarbrücken, Germany*

aegerter@inm-gmbh.de

*Received August 28, 2002; Accepted December 10, 2002*

**Abstract.** The paper reviews a low temperature sol-gel processing of transparent and antiglare conducting Sn doped indium oxide (ITO) coatings. The approach uses already crystalline nanoparticles which can be fully re-dispersed in an ethanolic sol containing a polymerisable organic binder. Thick single layers up to 600 nm can be deposited by spin and dip coating techniques followed either by a low temperature ( $<130^{\circ}\text{C}$ ) heat treatment or by a UV light irradiation. Stable resistivity down to  $9.5 \times 10^{-2} \Omega\text{cm}$  (sheet resistance of  $1.7 \text{ k}\Omega_{\square}$  for a 560 nm thick layer) have been obtained, together with high visible transparency ( $T \approx 87\%$ ), good adhesion (DIN 58196-K2, and 53151) and abrasion resistance (DIN 58-196 G10 and H25) and 1 H hardness. Irradiation through a mask allows to easily pattern the coatings. Antiglare-conducting coatings with adjustable gloss (60 to 80 GU) and maintaining a good optical resolution ( $>8$  lines/nm) were obtained by a conventional spraying technique. These techniques have been successfully applied to several plastic substrates such as polycarbonate (PC), polymethylmetacrylate (PMMA), polyimide, polyethylene (PE) as well as glasses.

**Keywords:** sol-gel, transparent conducting coatings, antiglare coatings, ITO, low temperature processing, nanoparticles, plastic substrates

## 1. Introduction

Transparent conducting oxide (TCO) coatings are today essential components in numerous applications when a high transmission is required in combination with a high electrical conductivity. Such coatings are therefore used as electrodes in photoelectronic devices, as IR reflecting or heatable layers, for electromagnetic shielding, for dissipating static, etc. [1, 2].

Wide band gap ( $E_g \geq 3 \text{ eV}$ ) n-type semiconductors such as tin doped indium oxide (ITO), antimony doped tin oxide (ATO) or aluminium doped zinc oxide (AZO) are among the most important and often used TCO materials. Such coatings are usually deposited by PVD (Physical Vapor Deposition) or CVD (Chemical Vapor Deposition) techniques [3]. These technologies

are rather costly but produce the lowest sheet resistance (typically  $10 \Omega_{\square}$ ) and adequate optical properties. Wet-chemical processing of TCO films is also a well adapted technique [4]. It is a low cost alternative especially if a low sheet resistance is not of prime importance. It allows to coat small to large flat substrates but also complex shaped substrates and cavities like tubes [5], difficult to obtain with the other techniques. Additionally, the excellent homogeneity and smoothness of sol-gel coatings can be used to smoothen rough surfaces [6].

Among the wet chemical processes to obtain TCO coatings, the most frequently used is the sol-gel processing. It is based on the hydrolysis of soluble metal precursors in solution of organic solvents like alcohols. The gel film deposited has however to be converted to an oxide film by subsequent drying and heat treatment steps at relatively high temperature. A similar approach

\*To whom all correspondence should be addressed.

is followed by metal-organic deposition (MOD) where the oxide film is formed by thermolysis of the dried precursor film. These two processes require therefore heat treatment steps at a temperature ranging from 400°C up to 1000°C to obtain good electrical, optical and mechanical properties [4]. Moreover these techniques do not allow to deposit thick layers and a low sheet resistance (the ratio of the specific resistivity to the thickness of the coating) can only be obtained by multilayers coatings, i.e. by repeating the whole coating procedure, a process not well adapted for industrial application. These techniques are therefore not adequate to coat substrates which do not withstand a posterior heat treatment like plastics and also glass devices already preshaped.

Only two "sol-gel" processes are reported in the literature to obtain transparent conducting coating, especially ITO ones, at low temperature.

A Japanese group [7–9] succeeded to crystallize at room temperature sol-gel ITO coatings deposited on plastics substrates by exposing them to a low fluence UV irradiation of an ArF laser (193 nm, 10–20 mJ/cm<sup>2</sup>). The surface temperature did not increase higher than 30°C. However the authors could only obtain a *conductivity* (typical resistivity of  $6 \times 10^{-2} \Omega\text{cm}$ , sheet resistance of about 6.6 k $\Omega_{\square}$ ) for coatings deposited on polyimide, polyethylene terephthalate (PET) and glass. The process failed for polycarbonate (PC) and polyethyl-ethyl-ketone (PEEK) substrates, as presumable microcracks are generated in these coatings by photodegradation of these substrates during the UV irradiation [8]. No comment on the mechanical properties of the layer has been reported.

A completely different route has been proposed by us and successfully worked out for many plastic substrates. The idea was to develop hybrid organic-inorganic sols containing the highest possible amount of already conducting crystalline oxide ITO nanoparticles [10, 11]. The major advantages of this technique are the separation of the crystallization step of the TCO material from the process of film formation on the one hand and the redispersability of the obtained nanoparticles in a variety of lacquer composition on the other hand. This offers the possibility of curing layers either by a low temperature thermal treatment (<130°C) or by UV light irradiation by using polymerisable organic additives [12, 13]. Also a high nanoparticles filling of the sol containing an adequate organic binder should assure a reasonable conductivity. The use of nanoparticles will lead to a low light scattering and to high

transparency of the coatings and, overall, the use of a hybrid sol should also favor the obtention of single thick coatings.

The paper reports on the state of the art of the preparation of ITO nanoparticles coatings at low temperature and their optical, electrical, mechanical and textural properties [12, 14–16].

## 2. Experimental

### 2.1. Precursors

In<sub>2</sub>O<sub>3</sub>:Sn crystalline nanopowders with primary size adjustable up to about 20 nm and having the cubic In<sub>2</sub>O<sub>3</sub> phase were prepared by a controlled growth technique. The detailed preparation can be found in [10, 11, 17, 18]. A solution of 0.5 mol indium (III) chloride in 1000 ml ethanol containing 8 mol% SnCl<sub>4</sub> (with respect to In) is added dropwise to an aqueous ammonia solution (25 wt%) containing  $\beta$ -analine. After a heat treatment at 80°C for 24 hours the resulting powder is isolated by centrifugation and then thoroughly washed with water. After a drying step at 60°C, the powder is annealed at temperature up to 350°C in a reducing atmosphere containing N<sub>2</sub> and H<sub>2</sub> (volume ratio 9 : 1). The so-obtained powders are crystalline with crystallite size up to 23 nm, a density of 6.67 g/cm<sup>3</sup> (95% of the theoretical density) and blue in color, indicating that they are conducting.

### 2.2. Sols

The powders are first mechanically redispersed in ethylene glycol with a carbon acid as dispersing agent. The so-obtained blue paste, with solid content up to 60 vol% is stable several months without evidence of agglomeration if a pH < 6 is maintained (pH<sub>iep</sub> = 8.5). Ethanolic solutions containing lower amount of ITO particles can be used for the obtention of thick coatings sintered at high temperature [15]. Figure 1 shows an HRTEM micrograph and the hydrodynamic particle size distribution of a sol prepared with powders heat treated at 350°C. A lower heat treatment temperature leads to smaller particle size.

To obtain conducting layers at low temperature, a small amount of a hydrolyzed binder such as 3-glycidoxypropyl trimethoxysilane (GPTS) or preferentially 3-methacryloxypropyl trimethoxysilane (MPTS) is added under ultrasonic agitation. A photostarter such as Irgacur 184 is also added to perform the

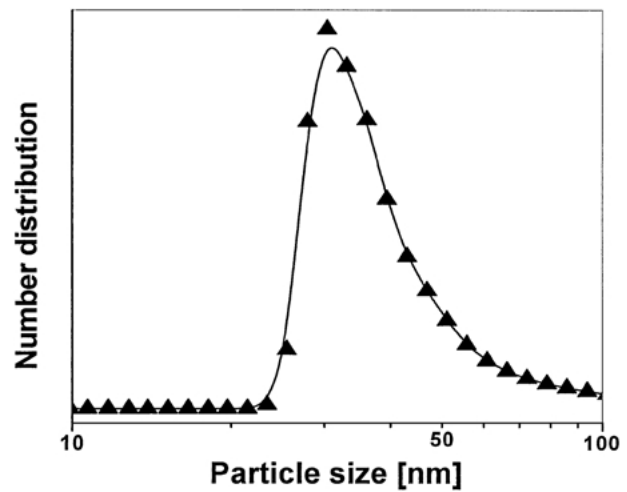
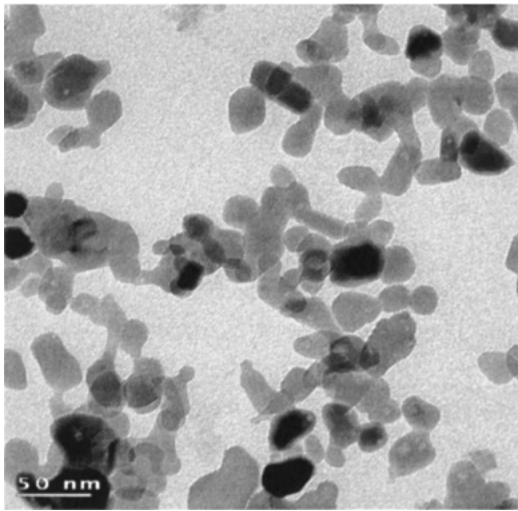


Figure 1. Left: HRTEM picture of crystalline  $\text{In}_2\text{O}_3\text{:Sn}$  nanopowder after annealing and redispersion in ethanol (pH 4). Right: typical ITO hydrodynamic particle size distribution in the suspension (from [16]).

polymerization of the binder. Such sols can be used for spin and dip coating conducting transparent layers or spraying conducting antiglare layers.

### 2.3. Coating's Process

Transparent coatings with thickness up to 600 nm have been obtained by spin or dip coating processes. Typical process parameters are 1000 rpm and 4 mm/s respectively. Substrates such as glass, PC, PMMA, PE, polyimide have been used. The best coating properties are obtained by first submitting the wet coating to a UV irradiation (typical average intensity 105 mW/cm<sup>2</sup> for 110 s (Beltron)) with a further heat treatment at 130°C up to 20 h. A post annealing under forming gas or N<sub>2</sub> atmosphere performed at 130°C during 2 h improves further the electrical properties.

Antiglare conducting coatings have been obtained by spraying the substrates with the same sols for a period of 15 to 20 s with a SMTA mini-jet gun (0.5 mm nozzle, 3 bar). The coatings have been further processed as described above.

### 2.4. Characterization of the Coatings

**2.4.1. Textural Properties.** The surface morphology of the coatings was analyzed using a white light interferometer (WLI) and AFM (Zygo Newview 5000) and Scanning Electron Microscopy (SEM-JEOL 6400).

Coating cross sections were observed by High Resolution Transmission Electron Microscopy (HR-TEM-Philips, 200 KeV).

**2.4.2. Optical Properties.** Optical transmission and reflection were determined using a Varian Cary 5 E spectrophotometer in the wavelength range 300 to 3000 nm. IR spectroscopy was performed with a Bruker IFS 66V instrument. Haze, clarity and gloss were measured using a ByK Gardner plus and a micro-TRI reflectometer.

**2.4.3. Mechanical Properties.** The thickness ( $t$ ) of the coating was determined using a Tencor P10 profilometer. The abrasion resistance of the coatings was tested according to DIN 58196—rubbing with a cloth (H25) or an eraser (G10) under a load of 9.8 N, the adhesion according to DIN 58196-K2 (tape test) and ASTM D 3359 or DIN 53151 (lattice cut test) and their hardness according to ASTM D3363-92a (pencil test).

**2.4.4. Electrical Properties.** The sheet resistance ( $R_{\square}$ ) was measured by a 4 points technique or a contactless measurement device (Lehighton Electronic Inc.). The resistivity was calculated from  $\rho = R_{\square} \cdot t$ . Carrier density and mobility were measured using a MMR van der Pauw equipment.

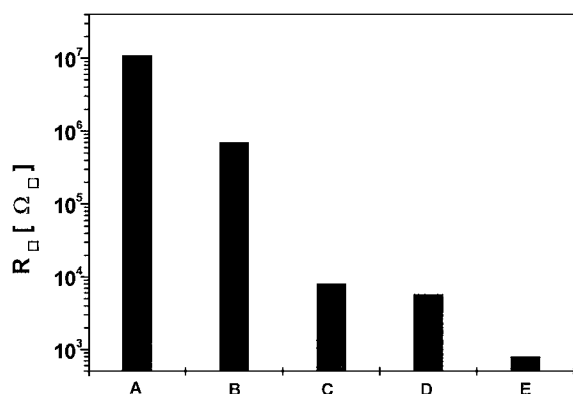


Figure 2. Sheet resistance of a 570 nm thick MPTS/ITO (6 vol%) coatings measured after different treatments in air. A: as deposited; B: as deposited + heat treatment in air at 130°C during 10 h; C: as deposited + UV irradiation (110 s, 105 mW/cm<sup>3</sup>); D: process C + heat treatment in air at 130°C/10 h; E: process D + reducing in forming gas at 130°C/2 h.

### 3. Results and Discussion

#### 3.1. Transparent Conducting Coatings

The lowest sheet resistance,  $R_{\square}$ , was obtained using a hybrid sol containing 6 vol% MPTS. The evolution of  $R_{\square}$  for a 500 nm thick single layer deposited on a 3 mm thick PC substrate is shown in Fig. 2. After a heat treatment at 130°C (process B), the sheet resistance is only reduced from  $10^7 \Omega_{\square}$  to about  $7 \times 10^5 \Omega_{\square}$ . However

if a UV treatment is performed (process C), the values drop down to  $8 \text{ k}\Omega_{\square}$  and to even lower values,  $6 \text{ k}\Omega_{\square}$ , if an additional heat treatment is performed (process D). A further annealing in a reducing atmosphere at 130°C during 2 h further decreases the sheet resistance to  $800 \Omega_{\square}$  (process E).

These variations are due to the different morphologies produced by these processes as shown by the HRTEM cross-sections of the coatings (Fig. 3). The right micrograph shows the morphology obtained after a heat treatment at 130°C (process B). The ITO particles are not bound together so that the sheet resistance is high. The left micrograph reflects the morphology obtained after UV irradiation and shows that the ITO particles are arranged in a compact and bound together by small strips of polymerized MPTS, leading to a higher conductivity. IR spectroscopy performed on a coating submitted to process D (Fig. 4) shows also that the C=C band at  $1630 \text{ cm}^{-1}$  is completely eliminated and that the C=O band at  $1716 \text{ cm}^{-1}$  is strongly reduced. The elimination of the organic groups is however not complete. This leads nevertheless to a well defined Si—O—Si network (band at  $1080 \text{ cm}^{-1}$ ) which links the conducting particles together. The UV treatment appears therefore fundamental.

The sheet resistance values have been measured immediately after the processing of the coatings and are stable if the layers are kept in vacuum or in a protective atmosphere (e.g. N<sub>2</sub>, Ar). Unfortunately,  $R_{\square}$  slightly increases slowly with time to reach a stable

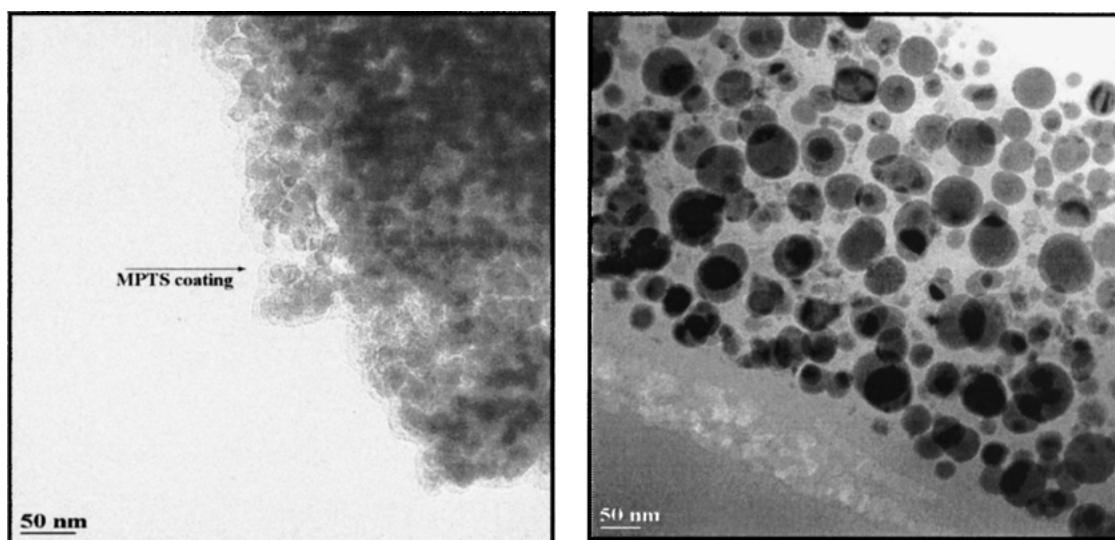


Figure 3. HRTEM cross-sections of ITO-MPTS coatings obtained after process B (right) and D (left).

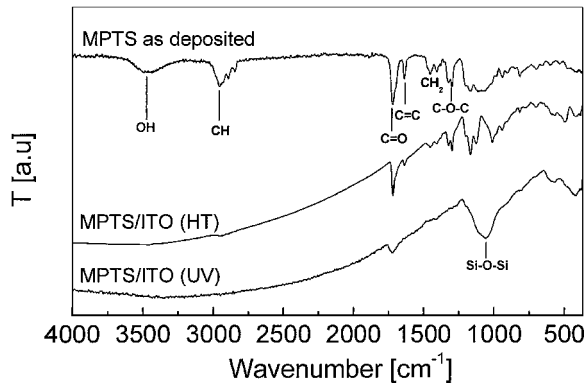


Figure 4. IR spectra of pura MPTS (as deposited) and MPTS/ITO coatings deposited on a Si wafer. HR: heat treated in air at 130°C, 15 h, UV: UV irradiated at 105 mW/cm<sup>2</sup>, 110 s (from [16]).

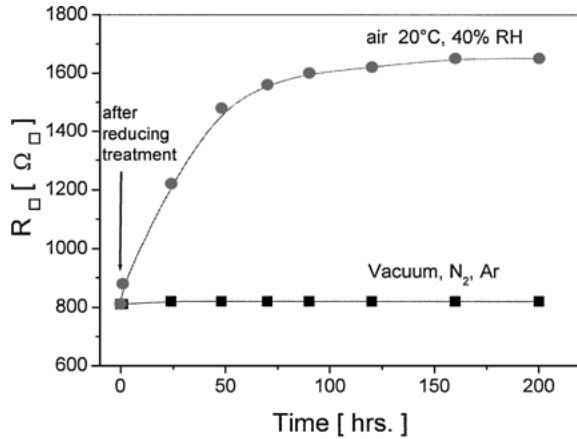


Figure 5. Time evolution of the sheet resistance of a 570 nm thick MPTS (6 vol%)/ITO coatings left in a protective atmosphere (vacuum, N<sub>2</sub>, Ar) and in air. The coatings have been initially post annealed in a reducing atmosphere (from [14]).

value of about 1.7 kΩ<sub>□</sub> in air (20°C, 40% RH) after about 7 days (Fig. 5). The process is reversible: a new short time UV irradiation of same intensity (105 mW/cm<sup>2</sup>, 120 s) allows to recover the lowest sheet resistance. This change of the sheet resistance during air storing depends on the thickness of the coating. The thicker the coating is, the smaller the variation is (Fig. 6).

The mechanisms leading to these variations are not yet clear. Besides the polymerization effect of the MPTS which bring and hold close together the ITO particles, the reversible change of  $R_{\square}$  in air involves primarily a decrease of the electron density  $n$  while the mobility of the electron only slightly decreases by

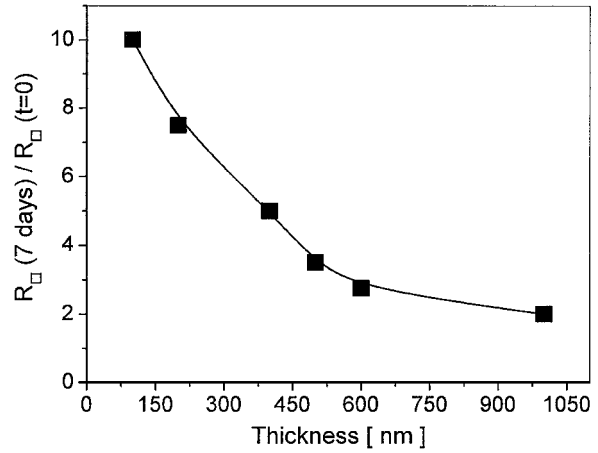


Figure 6. Ratio of  $R_{\square}$  measured after 7 days storing in air (20°C/40 RH) and immediately after the reducing treatment ( $t = 0$ ) versus the thickness of the coatings.

25%. The surface properties such as the work function, the contact angle (surface energy of the coatings) are also drastically affected [19]. Both the UV and reducing treatment are thought to diminish the concentration of chemisorbed oxygen species adsorbed on the surface of the ITO particles which act as free electrons surface state traps, enhancing the carrier concentration and consequently decreasing the sheet resistance. The back reaction, diffusion of O<sub>2</sub> species into the coating followed by a chemisorption at the ITO grains decreasing  $n$  and increasing  $R_{\square}$  is possible as the coatings are still porous.

The surface morphology of the coatings (process D, E) observed by SEM (Fig. 7) consists of loosely packed globular grains (raspberry like) about 100 nm in size formed by the aggregation of the ITO nanoparticles linked together by a small strip of polymerized MPTS (dark regions). The coating roughness measured by WLI on a 53 × 70 μm<sup>2</sup> area with a lateral resolution of 600 nm is  $R_a = 0.85$  nm, with a peak-to-valley maximum value of  $R_{PV} = 15$  nm. When measured with a higher resolution on a 1 × 1 μm<sup>2</sup> area (AFM), the values are  $R_a = 6$  nm.

The optical transmission and reflection spectra of a 3 mm thick PC substrate uncoated and one coated with a 500 nm hybrid ITO layer is shown in Fig. 8. A high transmission of about 87% is observed in the visible range. The influence of the carrier is clearly seen by the strong absorption occurring in the near IR range (900 nm <  $\lambda$  < 2000 nm) and the increase of the reflection for  $\lambda > 2$  μm.

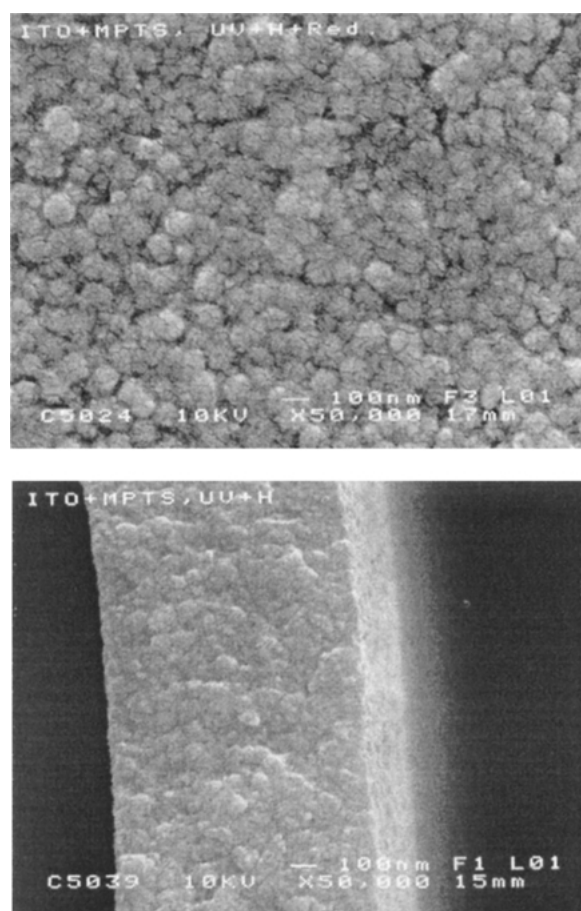


Figure 7. SEM picture of the surface (top) and HR-TEM cross-section (bottom) of a MPTS/ITO coating UV cured (110 s) and then heat treated at 130°C, 15 h (from [14]).

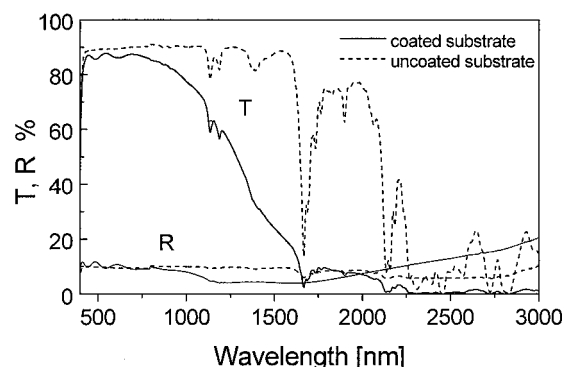


Figure 8. UV-near IR transmission ( $T$ ) and reflection ( $R$ ) measured against air of a 500 nm thick MPTS/ITO coating deposited on a 3 mm thick polycarbonate (PC) substrate and of an uncoated PC substrate (from [14]).

Table 1. Mechanical properties of transparent conducting ITO coatings deposited on a PC substrate.

Adhesion <sup>a</sup>	Adhesion <sup>b</sup>	Abrasion <sup>c,d</sup>		Hardness <sup>e</sup>
ok	Gt 0	Class 1 (b)	Class 1 (c)	1 H

<sup>a</sup>DIN 58196-K2.

<sup>b</sup>ASTMD 3359, DIN 53151.

<sup>c</sup>DIN 58196-H 25 (cotton).

<sup>d</sup>DIN 58196-G10 (eraser).

<sup>e</sup>ASTM D 3363-92 a (pencil).

The mechanical properties of the coatings deposited on PC substrate studied by various test are summarized in Table 1. The adhesion is in agreement with the Tape test procedure (DIN 58196-K2) and the result of the lattice cut test (ASTMD 3359, DIN 53151) is Gt 0 (the cutting edges are completely smooth). No scratch (class 1) was observed after 10 rubbing cycles with an eraser under a load of 10 N (DIN 58196-G10). The milder test rubbing with a cotton cloth (DIN 58196-H25) is also class 1 after 25 cycles. The hardness measured using the Pencil test ASTM D 3363-92a is 1 H. Higher values are obtained when the amount of MPTS is increased, but such coatings present also a higher value of the sheet resistance.

These mechanical properties are quite similar to those obtained with a commercial conducting polymer such as Baytron<sup>®</sup>P.<sup>1</sup> However, the transparency of the ITO coating in the visible range is far better, especially for thick coatings and the chemical and environmental stability are also much higher.

The coatings are easily patterned by selective UV irradiation using either a mask, a UV laser beam or UV holography. The exposed part strongly adheres to the substrate and the nonexposed part is easily washed in ethanol. Figure 9 shows a typical line pattern obtained by UV irradiation through a metallic mark placed directly on top of the wet coating.

### 3.2. Antiglare Conducting Coatings

Antiglare conducting coatings have been obtained by spraying followed by the same post deposition treatments. The spray gun delivers droplets with an average size of 25  $\mu\text{m}$ . When arriving on the substrate they spread and form a rough surface which can be polymerized following the same treatments (e.g. UV irradiation + heating at  $T \approx 130^\circ\text{C}$ ). The thickness of the coatings can range up to a few  $\mu\text{m}$ .

The surface morphology of such coatings consist of 10 to 100  $\mu\text{m}$  features with an average roughness of

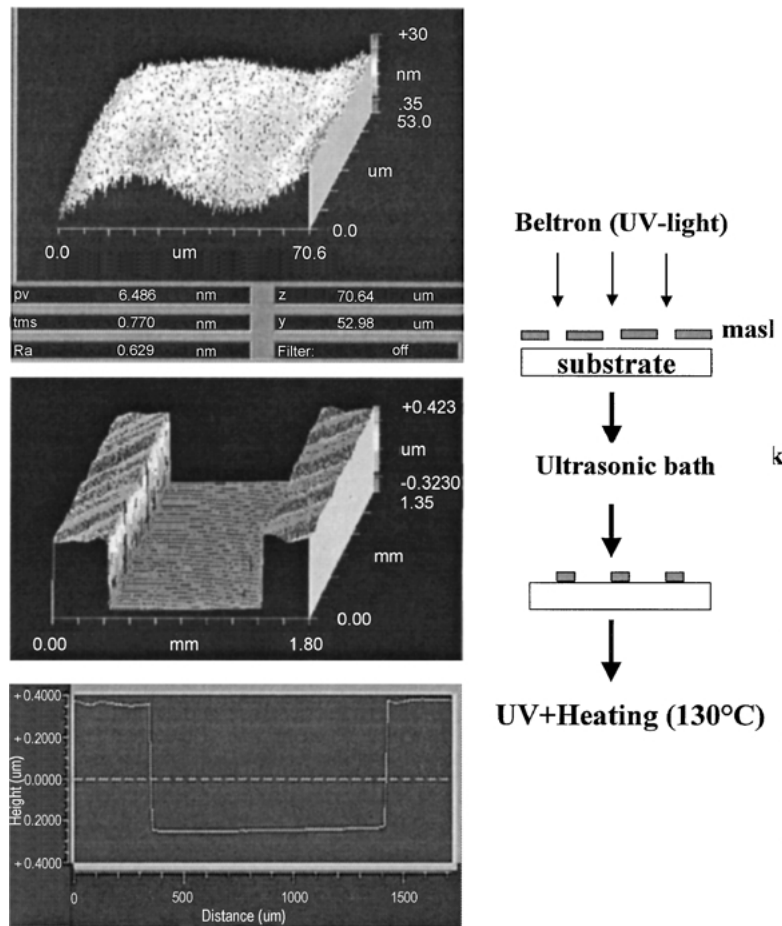


Figure 9. Line's pattern obtained by selective irradiation through a mask and removing the non-exposed area by washing in ethanol.

$R_a = 0.2 \mu\text{m}$  and peak to valley height of  $0.8 \mu\text{m}$  (Fig. 10). Similar sheet resistance values and mechanical properties similar to those obtained for transparent coatings have been obtained. Table 2 shows the results of the optical properties of the coatings.

Figure 11 shows the optical effect of such coatings. An image of the entrance of the INM building placed 2 cm behind a coated and a non-coated

Table 2. Typical gloss, haze, clarity, optical resolution and abrasion resistance of antiglare coatings cured by UV irradiation.

Gloss @ 60°	Haze (%)	Clarity (%)	Resolution (USAF chart)	Abrasion resistance (9.8 N) DIN 58196-G10
60–70	≤10	75–90	≥8 lines/mm	class 1

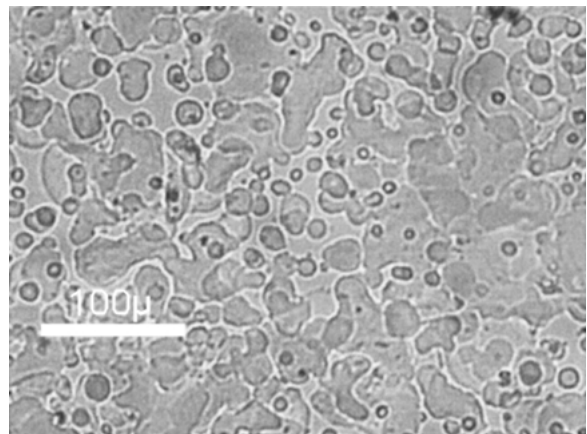


Figure 10. Surface morphology of antiglare coatings sprayed at room temperature on a PC substrate and UV polymerized.

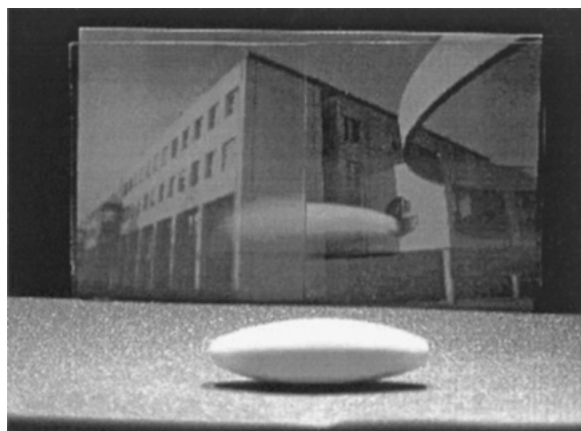


Figure 11. Glaze of a white object placed in front of a AS-AG coated plastic (left) and an uncoated one (right). The picture of the INM building placed 2 cm behind the substrates is clearly visible in both configurations.

substrate is clearly visible and the glare of the object placed in front of the coated substrate is strongly reduced.

#### 4. Conclusions

Stable hybrid pastes and sols allowing the deposition of conducting, antistatic and antiglare-antistatic coatings fully processable at low temperature ( $T < 130^{\circ}\text{C}$ ) have been developed. They have been obtained by modifying an ethanolic suspension of redispersed crystalline ITO nanoparticles with a hydrolyzed silane (MPTS) acting as a binder. Single layers as thick as about 600 nm have been obtained by spin or dip coating processes on plastic (PMMA, PC, PE, polyimide) and glass substrates. The best curing process involves a UV irradiation ( $105 \text{ mW}/\text{cm}^2$ , 110 s) followed by a heat treatment at  $T = 130^{\circ}\text{C}$  during 15 h and then a reducing treatment in forming gas. 570 nm thick coatings exhibit a high transparency ( $T \approx 87\%$ ) and a stable sheet resistance as low as  $1.6 \text{ k}\Omega/\square$  (resistivity  $\rho = 9 \times 10^{-2} \Omega\text{cm}$ ). The abrasion resistance is in agreement with DIN 58196-G10 class 1, the adhesion passes the tape test DIN 58196-K2 and the lattice cut test ASTM D 3359 or DIN 53151 and the pencil hardness according to ASTM D 3363-92c is 1 H. The surface roughness is low,  $R_a \approx 1 \text{ nm}$ .

Antistatic coatings with similar sheet resistance presenting an antiglare effect ( $\text{GU} \sim 65$ ) have been obtained on the same substrates by a spray process at

room temperature followed by UV irradiation and  $\text{N}_2$  annealing.

All these coatings are stable under UV or visible light irradiation and consequently their overall properties are already better than those obtained with commercial conductive polymers.

The process can be applied to coat conducting coatings at low temperature ( $T < 130^{\circ}\text{C}$ ) flat or slightly curved substrates such as CRT, LCD, PDP, touch screen panels, clean room discharge plates or bodies, plastic foils etc.

The concept of preparing crystalline ITO nanoparticles and to redisperse them into a polymerisable matrix is therefore quite adequate to obtain transparent or antiglare conducting coatings on plastic substrates and can be extended to other systems.

#### Note

1. Made by dip coating according to the Baytron<sup>®</sup> P Technical Information.

#### References

1. H.L. Hartnagel, A.L. Dawar, A.K. Jain, and C. Jagadish, *Semiconducting Transparent Thin Films* (Institute of Physics Publishing, Bristol, 1995).
2. B.G. Lewis and D.C. Paine, *MRS Bulletin* **25**, 22 (2000).
3. H.J. Gläser, *Large Area Glass Coating* (Von Ardenne Anlagentechnik GmbH, Dresden, 2000).
4. J. Pütz and M.A. Aegerter, in *Handbook on Sol-Gel Technologies for Glass Producers and Users*, edited by M.A. Aegerter and M. Mennig (Kluwer Publishers, Norwell, USA), in press.
5. J. Pütz, F.N. Chalvet, and M.A. Aegerter, in *Proc. Sol-Gel Optics VI*, Seattle, USA (SPIE, Bellingham, USA), **4804**, 73 (2002); *Proc. 76th Glastechnische Tagung*, Bad Soden, Germany, 2002, p. 334.
6. J.P. Cronin, A. Agrawal, and M. Trosky, Method for reducing haze in tin oxide transparent conductive coatings, US Patent no. 5900275 (1999).
7. H. Imai, A. Tominaga, H. Hirashima, M. Toki, and M. Aizawa, *J. Sol-Gel Sci. Technol.* **13**, 991 (1998).
8. H. Imai, A. Tominaga, H. Hirashima, and N. Asakuma, *J. Appl. Phys.* **85**, 203 (1999).
9. N. Asakuma, T. Fukui, M. Toki, and H. Imai, *J. Sol-Gel Sci. Technol.* **27**, 94 (2003).
10. D. Burgard, C. Goebbert, and R. Nass, *J. Sol-Gel Sci. Technol.* **13**, 789 (1998).
11. C. Goebbert, R. Nonninger, and H. Schmidt, Verfahren zur Herstellung von Suspensionen, Pulvern und Formkörpern von Indium-Zinn-Oxid, DE Patent no. 19840527 A1, 2000.



12. N. Al-Dahoudi and M.A. Aegerter, *Mater. Sci.* **20**, 71 (2002).
13. S.F. Kistler and P.M. Schweizer (Eds.), *Liquid Film Coating* (Chapman & Hall, London, 1997).
14. N. Al-Dahoudi and M.A. Aegerter, *J. Sol-Gel Sci. Technol.* (Proc. XIth Sol-Gel Workshop, Padova, 2001), **H26**, 693 (2003).
15. C. Goebbert, R. Nonninger, M.A. Aegerter, and H. Schmidt, *Thin Solid Films* **351**, 79 (1999).
16. N. Al-Dahoudi, H. Bisht, C. Goebbert, T. Krajewski, and M.A. Aegerter, *Thin Solid Films* **392**, 299 (2001).
17. C. Goebbert, M.A. Aegerter, D. Burgard, R. Naß, and H. Schmidt, in *Proc. Materials Research Society (MRS), Nanostructured Powders and their Industrial Application 1998*, vol. 520, p. 293.
18. C. Goebbert, M.A. Aegerter, D. Burgard, R. Naß, and H. Schmidt, *J. Mater. Chem.* **9**, 253 (1999).
19. N. Al-Dahoudi and M.A. Aegerter, to be published.